

Beam Dynamics Study for TESLA with the Integrated FEL

V.M. Tsakanov

Yerevan Physics Institute, Alikhanian Br. 2,
375036 Yerevan, Armenia

Contents

1	Introduction	2
2	The smoothly curved orbit (CDR)	3
2.1	Linear optic	4
2.2	Emittance preservation	7
2.3	Conclusion 1	10
3	The TESLA high luminosity	11
3.1	Linear optics	13
3.2	Free coherent oscillations. Dispersive effects	14
3.3	Free coherent oscillations. Wakefield effects	15
3.4	Accelerator section misalignments	16
4	Trajectory correction	18
4.1	One-to-one correction	18
4.2	Two beam operation	20
4.3	On the two beam based trajectory correction	22
5	Summary	25

1 Introduction

In the TESLA project, part of the main linac will be used to accelerate the beam for the integrated X-ray Free Electron Laser (FEL) facility. The beams for high energy physics and FEL have different requirements and correspondingly have different energies, emittances, bunch charge and length. Both beams are assumed to accelerate in the first part of the linac in an interleaved pulse mode, where RF pulses for high energy physics and those for X-ray physics alternate.

The TESLA beam dynamics, including the preliminary consideration of the two-beam operation mode, is given in the Conceptual Design Report (CDR) [1]. The study presented in this report is basically related to beam dynamics in two-beam operation mode.

We start with the beam dynamics in the first part of the main linac with the existing design (CDR) when the orbit is smoothly vertically curved with a bending radius of 915 km to level an 8 mrad tilt of the existing ring HERA to enable the option for producing collisions of protons stored in HERA with electrons from the main linac. The main features of the machine linear optic are then two dispersions and two separate design orbits related to the TESLA and FEL beams. In addition, with two different energies of the beam, the use of one-to-one correction technique for high energy beam is accompany by large coherent oscillations of the low energy FEL beam leading to emittance grow. The application of the beam based trajectory correction in curved part of the linac also becomes problematic due to large dispersion of the TESLA beam and separate design orbit of the FEL beam.

Therefore, the modified approach is given based on the local bend of the 55 GeV high energy TESLA beam on about 8 mrad to adjust the design trajectory with the horizontal direction of the main linac. The two-beam operation part of the main linac is then straight and effects caused by the curved orbits vanish. With the new design, the main aspects of the beam dynamics with regards on emittance preservation for both beams are given including the wide-band energy option of the FEL and TESLA beams with the reduced vertical emittance of the high luminosity TESLA beam. Some features of the trajectory correction in two beam operation part of the main linac are discussed.

2 The smoothly curved orbit (CDR)

The Linear Collider will be built underground at a depth of about 15 m. The interaction point HERA west is about 20 m above sea level. The axis of the main part of the linac tunnel lies about 10 m below sea level. The straight section HERA West has a slope of about 8 mrad out of the horizontal. Therefore, to enable the option for producing collisions of protons stored in HERA with electrons from the main linac, there is a transition from the initial slope into the horizontal direction of the electron beam. Fig.1 shows an expanded profile of the linear collider area North-Northwest of DESY together with the collider tunnel. The two possibilities of the transition from the initial slope into the horizontal direction are the smooth curve by the corrector dipoles and the local bend of the TESLA beam (at energy about 50 GeV) by the achromat section. Note, that the machine performance (the tunnel and the cells arrangement) in this part of the linac is basically determined by the beam dynamics in two-beam operation mode. Although, the different aspects of the beam dynamics for single TESLA and TESLA/FEL beam operations are given in CDR, there are some peculiarities in two-beam operation mode which impose a certain constraints on the machine performance and trajectory correction procedure.

In this section we give some aspects of the beam dynamics in two-beam operation mode when the design orbit of the TESLA beam is smoothly curved with a bending radius of about 1000km as is shown in Fig1.

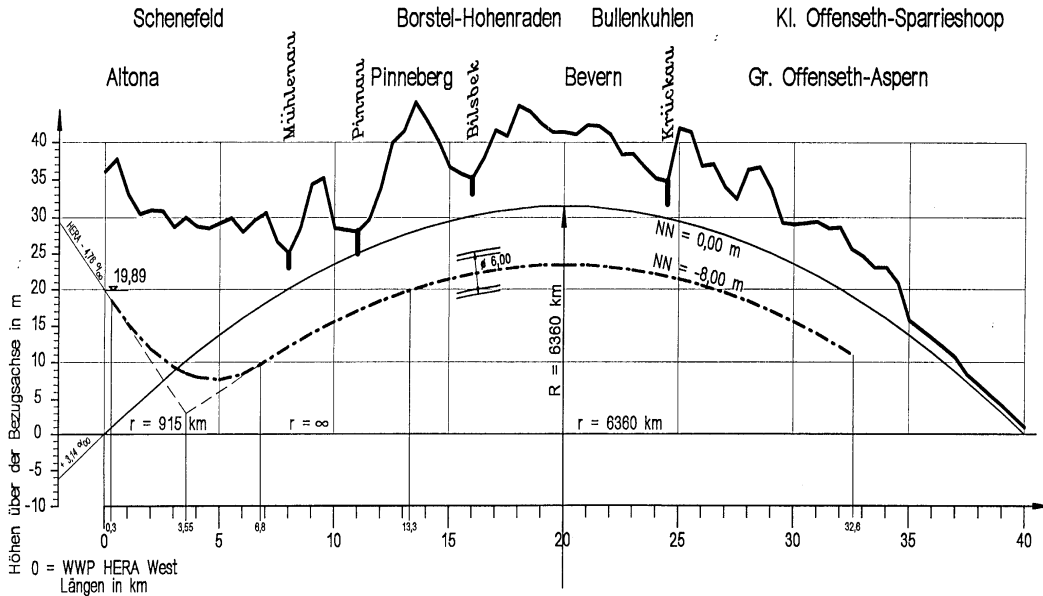


Fig.1 Expanded profile of the Linear Collider area North-Northwest of DESY.

2.1 Linear optic

The linear optic design of the TESLA main linac is based on low phase advance per single FODO cell $\mu_T = 60^\circ$. To accelerate in FEL mode with a gradient close to the most efficient one of $U_F = 18 \text{ MeV/m}$ keeping the constant ratio of TESLA and FEL beam energies $E_F/E_T = U_F/U_T = 0.72$, the phase advance of the FEL beam in thin lens approximation is given by

$$\sin(\mu_F/2) = \frac{U_T}{U_F} \sin(\mu_T/2) \quad (1)$$

and is approximately equal to $\mu_F = 90^\circ$. The injection energies of the TESLA and FEL beams are then 3.2 and 2.3 GeV respectively. Note, that beyond some energy offset, no optical solution exists any more for a periodic FODO lattice. For the TESLA lattice this occurs at about 40% of the linear collider operation gradient. The periodic betatron functions for TESLA and FEL are shown in fig.2.

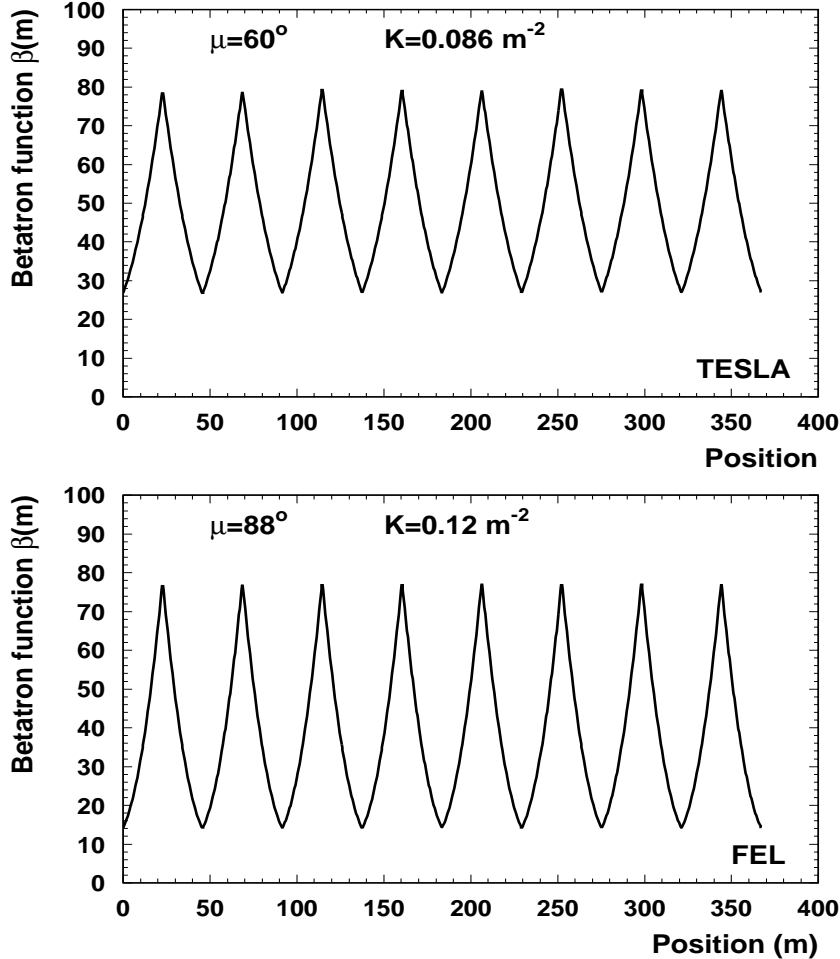


Fig.2 *The betatron functions of the TESLA and FEL beams.*

The phase ellipses of injected beams for TESLA and FEL operations have to be matched with machine ellipses to prevent the emittance dilution of the beta-mismatch [3]

$$\frac{\Delta\varepsilon}{\varepsilon} = \frac{1}{2} \left[\frac{\beta}{\beta^*} + (\alpha - \alpha^*)^2 \frac{\beta^*}{\beta} + \frac{\beta^*}{\beta} \right] \quad (2)$$

where α, β machine initial Twiss parameters, α^*, β^* the Twiss parameters at the end of injection channels. As an example, if the matching point is at the middle of the quadrupole ($\alpha = 0$), for the 5% of emittance dilution we get

$$\alpha^* \leq 0.22, \quad 0.75 \leq \frac{\beta^*}{\beta} \leq 1.27 \quad (3)$$

To estimate the effect of the curved TESLA beam trajectory in the first path of the linac, we assume that the design orbit is smoothly curved by the dipole corrector magnets. The number of FODO cells in the curved part of the linac is approximately 160 and each magnet deflect the design trajectory by the angle of about 0.05 mrad with the bending radius for TESLA beam about 10 km (one magnet per cell). The off-energy trajectories of the FEL and TESLA beams in the two beam operation part of the linac is then given by two dispersions. The periodic dispersion functions for the TESLA and FEL beams are shown in Fig.3. Note, that the required magnetic field of the corrector dipoles with the TESLA beam energy 140 GeV is then close to maximum field of 44 mT [1].

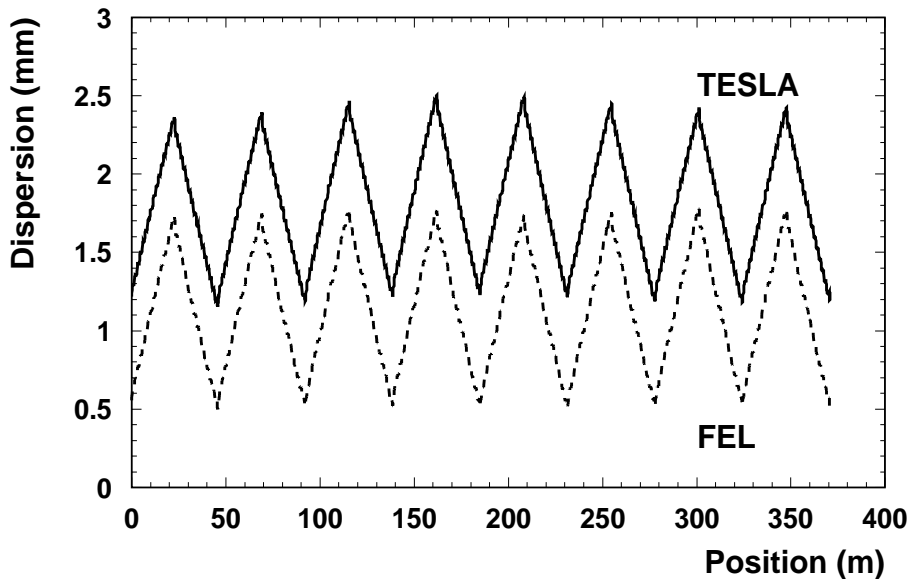


Fig.3 The periodic dispersion functions for the TESLA (solid line) and FEL (dashed line) beams.

In addition, the low energy FEL beam central trajectory is given by

$$y_F'' + \frac{\gamma'}{\gamma} y_F' + K_F y_F = \left(1 - \frac{E_T}{E_F}\right) G_T \quad (4)$$

with the neglect of nonlinear term $GK y^2$. Here $G = 1/\rho$ is the bending curvature, K the quadrupole strength. It can be shown, that the periodic solution of the equation of motion (4) is then define the design orbit of the FEL beam in TESLA (Fig.4a). Note, that the design orbit of the FEL beam is not follow to off-energy trajectory of the TESLA beam and has a reduction factor of about two due to high betatron phase advance of the FEL beam. Actually, the FEL beam central trajectory is the periodical solution if the bunch center position is matched with the initial amplitudes y_0, y_0' of the design orbit. For comparison, Fig.4b presents the FEL beam coherent oscillations when the beam is injected along the axis of the main linac with the zero initial amplitudes.

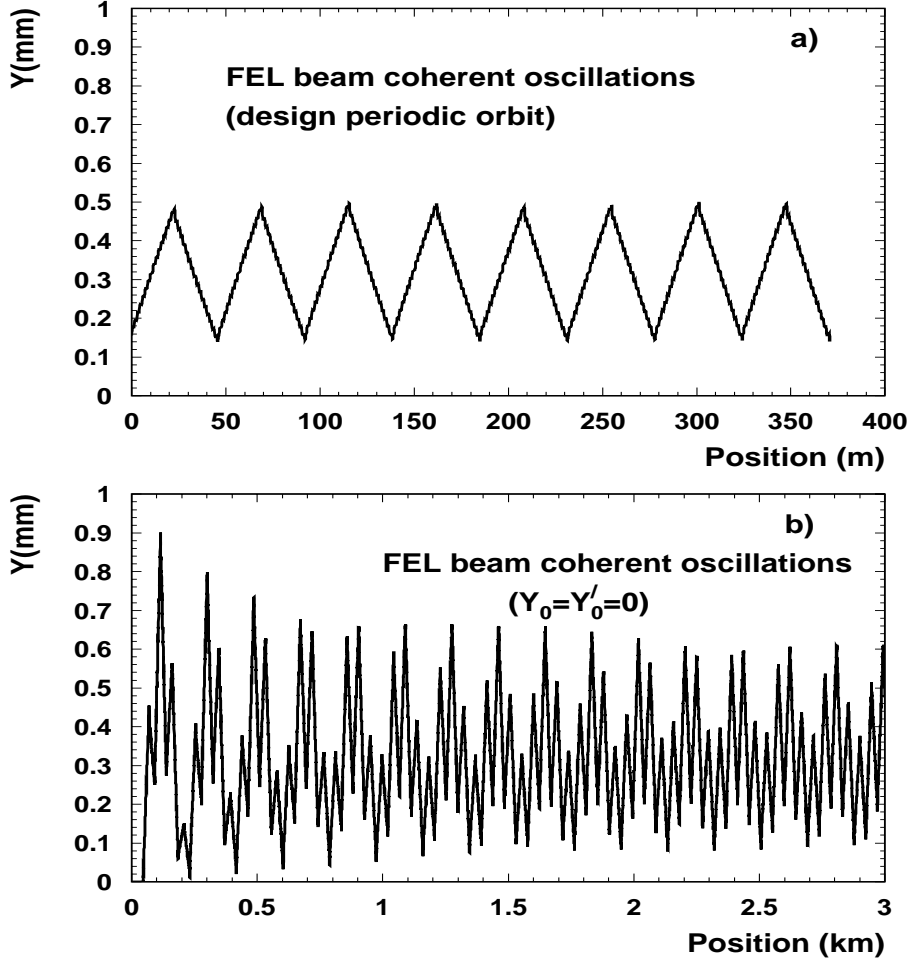


Fig.4 The FEL beam design periodic orbit (a) and the coherent oscillations of the beam with initial zero amplitudes (b)(on axis injection).

2.2 Emittance preservation

In this section some aspects of the dispersive and wakefield caused emittance dilution of the FEL and TESLA beams is given based on the CDR[1].

a) *Dispersive effects. Coherent oscillations*

Fig.5 shows the emittance dilution of the TESLA and FEL beams caused by injection jitter and initial uncorrelated energy spread δ_0 . The beams perform coherent betatron oscillations with one sigma initial offsets with respect to design orbits. For comparison, the dispersive emittance dilution of the FEL beam is shown when the beam is injected along the axis of the main linac. Thus, to stabilize the emittance dilution of the FEL beam with the accuracy better than 5%, the uncorrelated energy spread limited by 1% and the injection jitter by one sigma offset with respect to FEL design orbit.

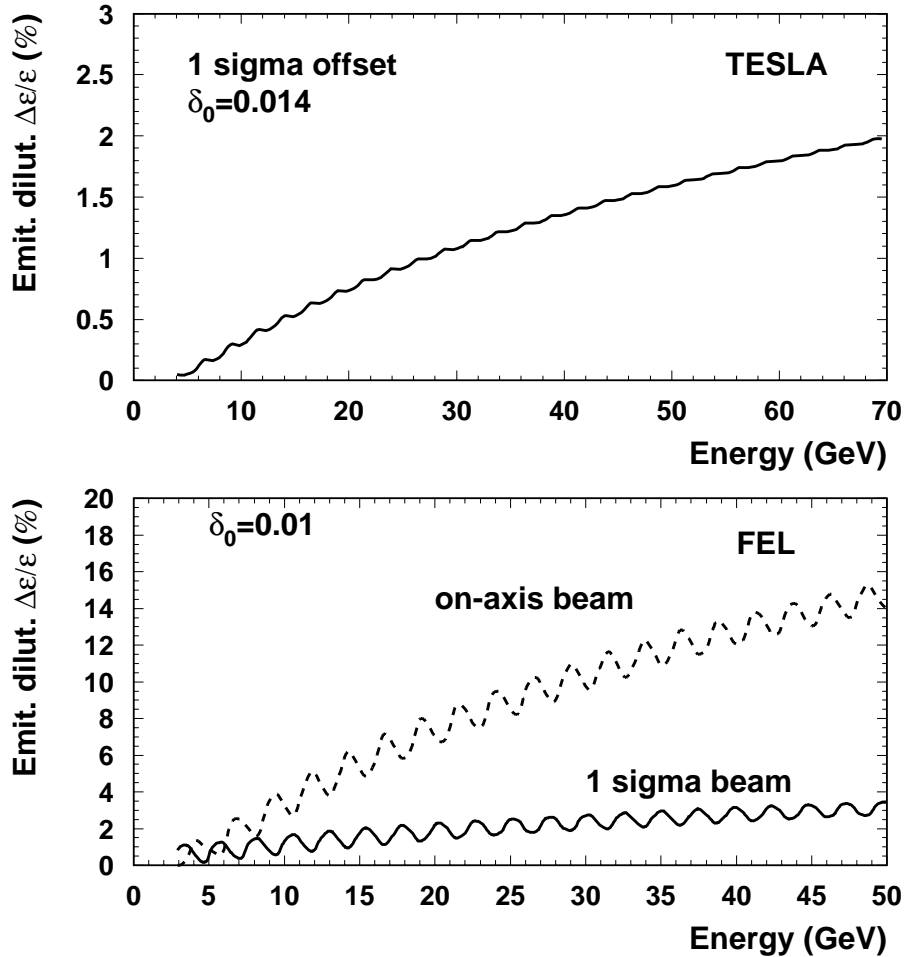


Fig.5 The uncorrelated dispersive emittance dilution of the TESLA and FEL beams. Shown are the cases of one sigma initial offset (solid lines) and on-axis injected (dashed line) FEL beam.

b) *Wake field effects.*

The wake fields caused emittance dilution of the TESLA and FEL beams is shown in Fig.6. The high energy TESLA beam performs coherent betatron oscillation with one standard initial offset. For the FEL beam are shown the cases when the beam is follow the design orbit (matched beam) and the beam injected on the axis of the main linac. The effect is in order of few percent for TESLA beam and negligible (in order of 10^{-4}) for FEL beam. Note, that the dominant contribution to emittance dilution of FEL beam is caused by the longitudinal wakefields.

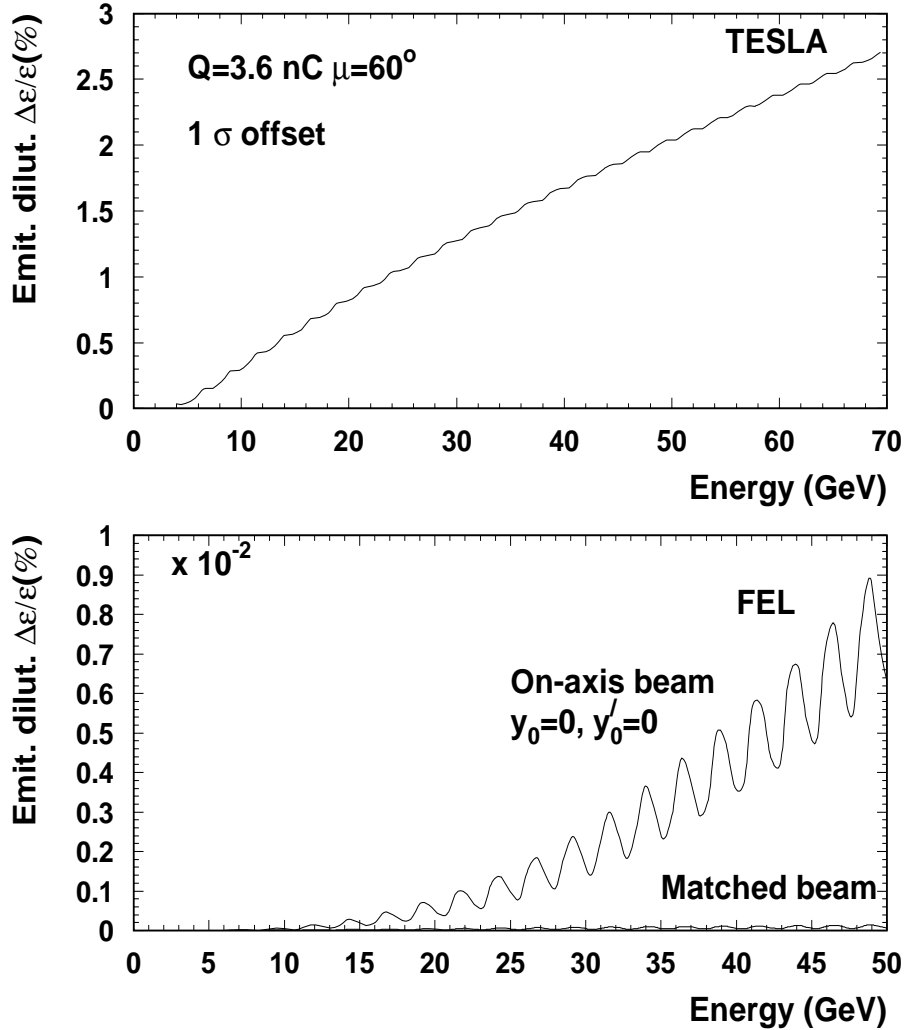


Fig.6 *The wake field emittance dilution of the TESLA and FEL beams. For the FEL beam the matched and on-axis injected beams are shown.*

c) *Trajectory correction*

The quadrupole misalignments of the linac affect both trajectories of the TESLA and FEL beams. Note, that if the trajectory of one of the beams is corrected, the second beam with the large energy deviation $\bar{\delta}$ experiences an additional kick in quadrupoles that contain the lattice. The kick is proportional to the corrected trajectory offset of the first beam and is given by $\Delta y'_2 \sim \bar{\delta} K L_q y_1$. Thus, the second beam is not follow the dispersion trajectory and performs additional beating, the amplitude of which can substantially grow leading to large emittance growth. We will return to this problem in the next section. Fig.7 shows the TESLA and FEL beams trajectories when the high energy beam is corrected by using one-to-one correction technique. Note, that the dispersion functions are exactly follow the trajectories of the beams.

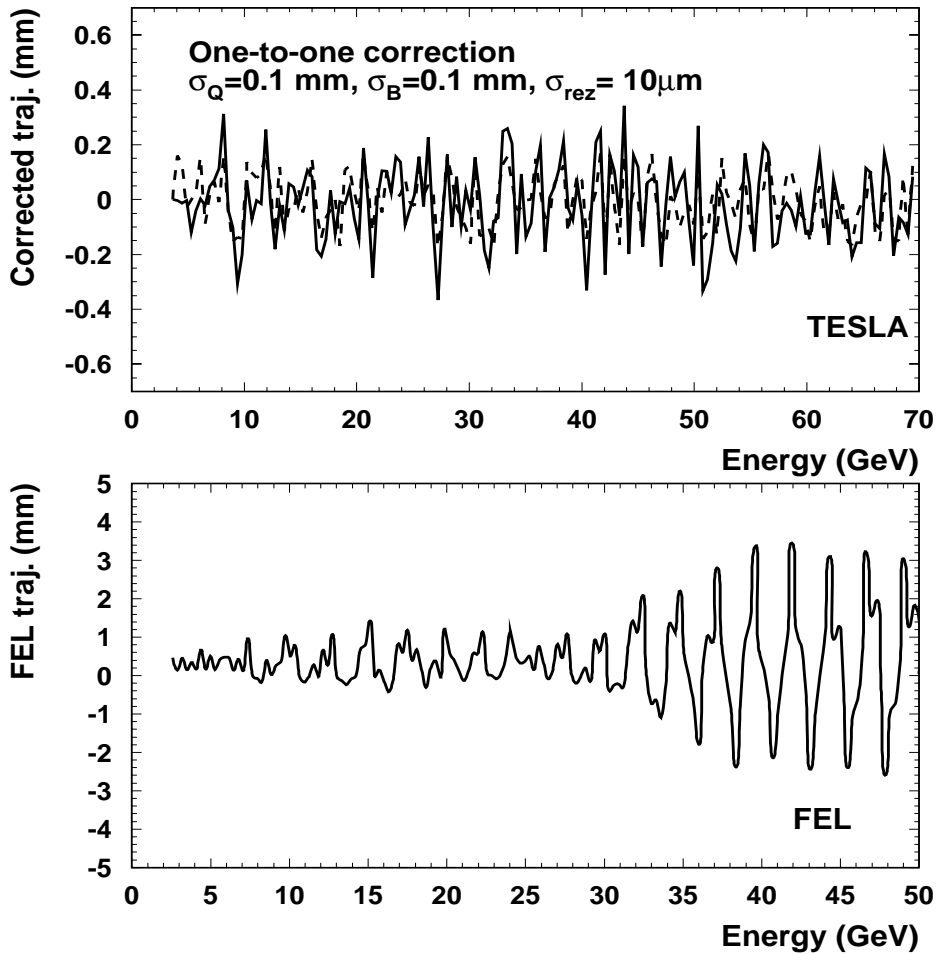


Fig.7 *The beating of the FEL beam with one-to-one correction of the TESLA beam. Shown the quadrupole misalignments-dashed line, the TESLA one-to-one corrected trajectory-solid line (top) and the coherent oscillations of the FEL beam (bottom).*

2.3 Conclusion 1

The results of this section with the study outlined in the Conceptual Design Report show that the operation of the machine with the smoothly curved design orbit can be proceeded with emittance preservation for both beams at the level of better than 10% by the separate one-to-one trajectory correction of the TESLA and FEL beams. Otherwise, the one-to-one correction of the TESLA beam only leads to large coherent oscillations of the FEL beam and the beam-based trajectory correction technique should be in used to prevent the emittance enlargement of the FEL beam. Note, that an application of the beam based correction procedure supposes the information about on- and off-energy beam trajectories, which, in turn, includes an additional errors due to separate beam trajectories and dispersions.

Summarizing the main aspects of the beam dynamics study in the smoothly curved machine, the following main disadvantages can be listed.

Beam dynamics:

- * the FEL beam should be matched with the design orbit to prevent the emittance dilution of injection jitter;
- * the dispersions of the TESLA and FEL beams should be matched to obtain the minimum periodic dispersion of the machine;
- * the application of one-to-one correction technique in two-beam operation mode is excluded due to large coherent oscillation of the FEL beam;
- * the periodic dispersion is still large (2.5 mm) and the application of the beam based trajectory correction becomes problematic due to additional sources of the errors.

Machine performance:

- * an each FODO cell should be geometrically curved by about 0.05 mrad to be linked with the design trajectory of the TESLA beam; in turn, the each cell should be aligned with the accuracy better than $100\mu m$;
- * the option of the further colliding of the TESLA electron beam with HERA proton beam needs some reconstruction of the machine elements as far as the correction dipoles with the maximum magnetic field 44 mT could not provide the corresponding bend of the electron beam at energies 200-250 GeV.

To prevent all these disadvantages of the machine performance and beam dynamics issues, the part of the main linac with parallel operation of collider and FEL beams is reasonable to be straight with further local bend of the collider beam in achromat cell after the separation of collider and FEL beams (Fig.1). The energy of the collider beam is then at the level of 55 GeV . The FEL beam is extracted from the linac at the different energies (15, 25 and 50 GeV) by the fast kicker setup and is transported to the user laboratories.

3 The TESLA high luminosity

As it is shown in the previous section, the reasonable solution for the transition of the collider beam to horizontal direction (the two-beam operation part of the main linac) is the local bend of the high energy TESLA beam after the separation of the FEL beam. An additional argument for this option is the new high luminosity parameter set of the TESLA beam with the injection energy at the level of the 5 GeV [3, 4]. The parameter list for FEL and high luminosity TESLA beams is given in Table 1.

TABLE 1

Parameters	TESLA	FEL
Injection energy (GeV)	5	2.2
Vertical emittance ($mm \cdot mrad$)	0.03	0.7
Charge per bunch (nC)	3.2	1
Bunch rms length (mm)	0.4	0.025
Accel gradient (MeV/m)	25	18

The local bending section for the TESLA beam is started at the horizontal position 3.55 km (Fig.1) when the high energy TESLA beam reaches the energy 55 GeV. The focusing cells arrangement of the TESLA main linac is given in CDR report. The linac is divided into 3 sections, with quadrupole spacing of 2, 3 and 4 cryo-modules, respectively. The first beta-step (change of the optics) is at the level of 55 GeV. Thus, the achromat cell includes the additional quadrupole section for betatron matching. The layout of the achromat bending cell with the betatron matching section is shown in fig.8.

The minimum bending radius of the TESLA beam is defined by the emittance growth of the 200 GeV electron beam (the electron-proton collision option with 250 GeV electron beam) caused by incoherent synchrotron radiation. In a transport line, the emittance growth ($\Delta\varepsilon/\varepsilon \ll 1$) due to incoherent synchrotron radiation can be estimated by [5]

$$\Delta(\gamma\varepsilon)[m \cdot rad] \approx 4.13 \cdot 10^{-8} E^6[GeV] I_5[m^{-1}] \quad (5)$$

where E is the beam energy in GeV and I_5 is the fifth synchrotron integral

$$I_5 = \int_0^L \frac{G^3}{\beta} \left[\eta^2 + \left(\beta\eta' - \frac{1}{2}\beta'\eta \right)^2 \right] ds \quad (6)$$

with $G(s) = 1/\rho(s)$, ρ is the bending radius, L is the total length of the transport line. For the maximum emittance growth $\Delta(\gamma\varepsilon) \approx 10^{-7} m \cdot rad$ at the beam energy 200 GeV, the estimated bending radius is in order of 5 km (magnetic field 0.1334 T). The total length of the bending magnets is then 40 m with deflection angle of 8 mrad.

The evaluation of the betatron and dispersion functions of TESLA along the transition transport line is shown in Fig.8. The two bending magnets B and the triplet T3 (q3,q4,q5) provide the achromat bend of the 55 GeV TESLA beam by an angle of 8 mrad. The length of the bending magnet is 20 m with the magnetic field 36 mT. The two end quadrupole doublets D1(q1,q2) and D2(q6,q7) provide the matching of the optical functions between section one and section two (first beta-step) and allowed to obtain an optimal beam envelope along the transport line. The quadrupole strengths that provide a complete matching of the Twiss parameters for a phase advance per cell $\mu = 60^\circ$ are given in Table 2. The positive and negative values of the strength are related to defocusing and focusing quadrupoles in horizontal plane. The length of quadrupoles is 0.5m and the total length of the transition transport line is 51 m. The fifth synchrotron integral of the transport line is equal to $I_5 = 1.35 \cdot 10^{-13} m^{-1}$.

TABLE 2

Quadrupoles	q1	q2	q3	q4	q5	q6	q7
Strength (m^{-2})	0.40	-0.38	-0.41	0.95	-0.41	-0.32	0.38

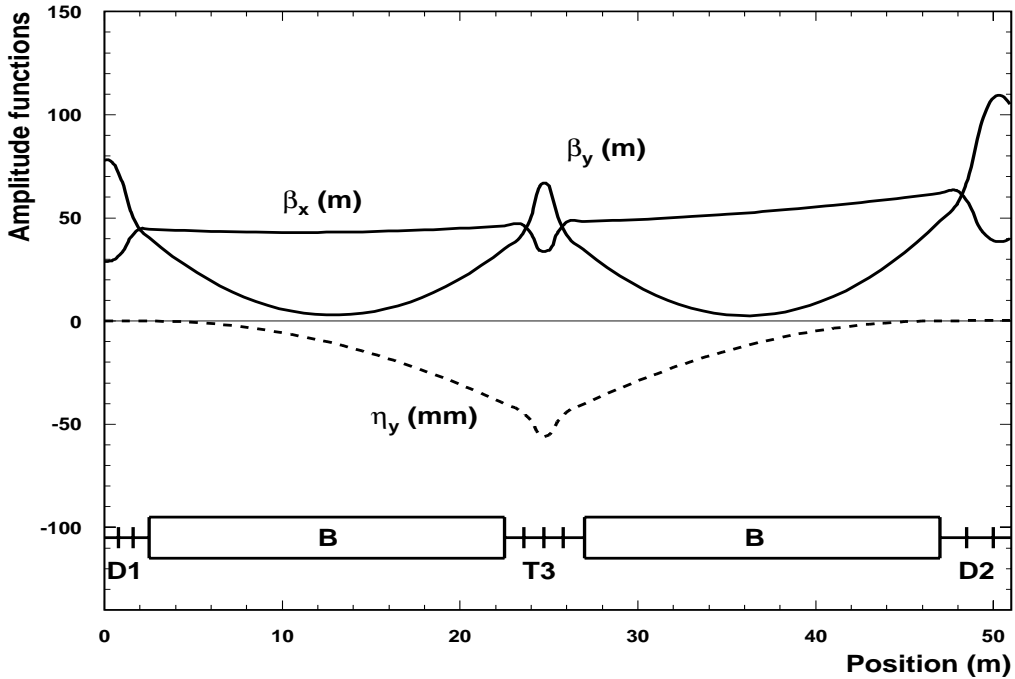


Fig.8 *The betatron and dispersion functions in achromat matching section*

3.1 Linear optics

The optical solution for two beams with different initial energies to be accelerated at the same FODO beamline is approximately given by the modified formula

$$\sin(\mu_T/2) = \sin(\mu_1/2) \left(\frac{E_{0T} E_F(n)}{E_{0F} E_T(n)} \right)^\alpha \quad (7)$$

$$\sin(\mu_F/2) = \sin(\mu_{1T}/2) \left(\frac{E_{0T}}{E_{0F}} \right)^\alpha \left(\frac{E_T(n)}{E_F(n)} \right)^{1-\alpha} \quad (8)$$

where E_0 is the initial energy of the beam, μ_n is the phase advance in the n -th FODO cell, $E(n) = E_0 + U \cdot n$ is the energy at the entrance of the n -th cell, U is the acceleration gradient, α is the scaling parameter and subscript (T,F) indicates the TESLA and FEL beams respectively. The nominal focusing regime for both beams is then given by the form.(1) and is reached at the energy of about 20 GeV of a TESLA beam (about 20 cells).

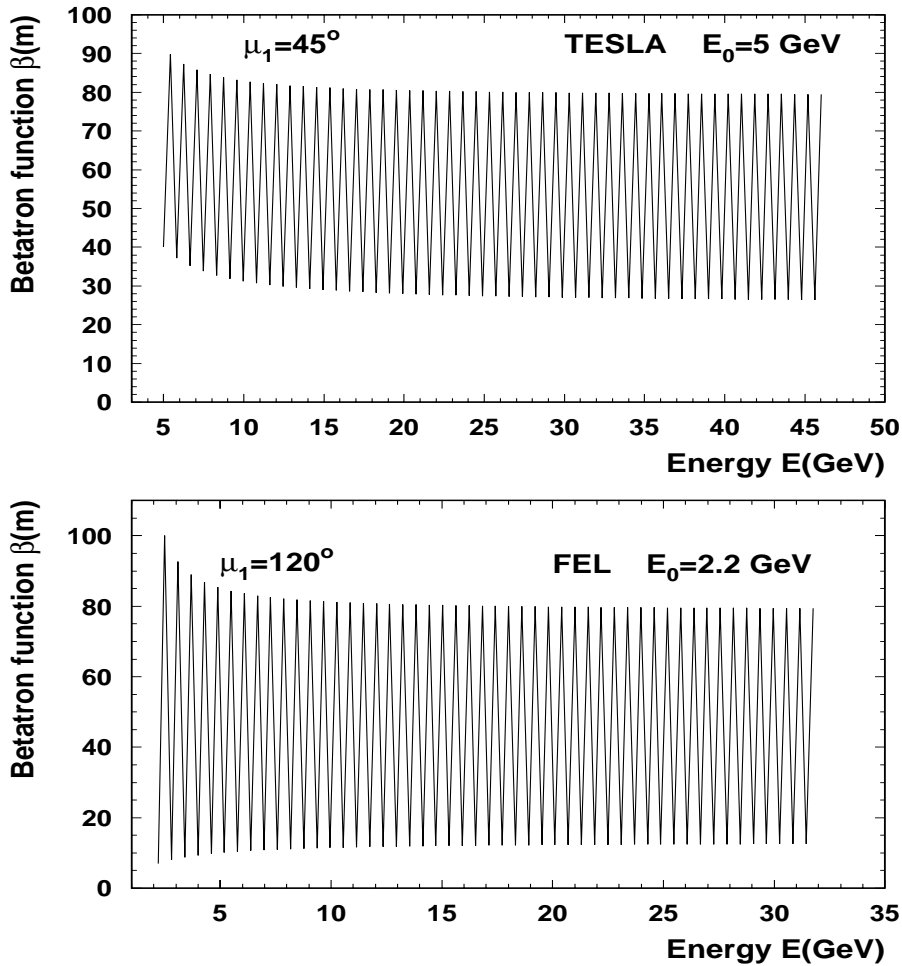


Fig.9 The betatron functions for the TESLA and FEL beams.

For the injection energies $E_T/E_F = 5/1.5$, the compromise solution for both beams is $\alpha = 0.85$ with the phase advance per first cell for TESLA beam $\mu_{1T} = 30^\circ$ and for FEL beam $\mu_{1F} = 119^\circ$. Actually, the relation of the injection energies 5/1.5 (GeV) is the limiting case since the further decreasing of the FEL beam energy accompany by the strong wakefield emittance dilution (scales as $\sin^{-2} \mu$) of the TESLA beam and strong dispersive emittance dilution (scales as $\tan^2 \mu/2$ of the FEL beam).

Therefore, we focus on the reasonable injection energy relation 5/2.2 (GeV) of the TESLA and FEL beams with the optimal scaling parameter $\alpha = 0.6$. The phase advance per FODO cell for TESLA beam is then slightly increase from 45° up to nominal value 60° , while the phase advance for the FEL beam decreases from 120° to nominal value about 90° . Thus, the TESLA beam betatron function envelope at the end of the first section of the machine is coincide with the CDR. Fig.9 shows the variation of the betatron functions along the linac for TESLA and FEL beams.

3.2 Free coherent oscillations. Dispersive effects

The dispersive emittance dilution of the beam in linear accelerator that is caused by coherent betatron oscillations and particle energy spread is well known and is given by

$$\Delta\varepsilon = \frac{1}{2}a_0^2 \frac{\gamma_0}{\gamma} \left(1 - \frac{\sin^2 \Delta\mu}{\Delta\mu^2}\right) \quad (9)$$

where a_0^2 is the area of the machine initial phase ellipse (divided by π), γ_0, γ the initial and actual Lorenz factors of design particle, $\Delta\mu$ the betatron phase shift of the off-energy particle. The phase shift of off-energy particle is caused by correlated and uncorrelated energy spreads, and in constant beta lattice machine ($\mu = const$) is given by

$$\Delta\mu_{un} = 2\delta_0 \tan \frac{\mu}{2} \frac{\gamma_0}{\Delta\gamma} \ln \frac{\gamma_0}{\gamma} \quad (10)$$

$$\Delta\mu_{cor} = 2\delta_c \tan \frac{\mu}{2} \frac{\gamma_0}{\Delta\gamma} \left(\frac{\gamma}{\gamma_0} - \ln \frac{\gamma}{\gamma_0} - 1 \right). \quad (11)$$

The corresponding emittance dilutions of the beam with one standard initial offset in low chromaticity machine ($\Delta\mu \ll 1$) are then approximately given by

$$\frac{\Delta\varepsilon}{\varepsilon_{un}} = 2\delta_0^2 \tan^2(\mu/2) \left(\frac{\gamma_0}{\Delta\gamma} \right)^2 \ln^2 \frac{\gamma(z)}{\gamma_0} \quad (12)$$

$$\frac{\Delta\varepsilon}{\varepsilon_{cor}} = 2\delta_c^2 \tan^2(\mu/2) \left(\frac{\gamma_0}{\Delta\gamma} \right)^2 \left(\frac{\gamma}{\gamma_0} - \ln \frac{\gamma}{\gamma_0} - 1 \right)^2. \quad (13)$$

where δ_0, δ_c are the rms initial uncorrelated and actual correlated energy spread of the beam, $\Delta\gamma$ the energy gain per FODO cell.

Fig.10 shows the results of the tracking simulation for TESLA and FEL beams with one standard initial offsets and initial uncorrelated energy spread $\delta_0 = 0.01$. For comparison shown also the analytical prediction of the emittance dilution for a TESLA beam with a constant phase advance $\mu = 60^\circ$ per cell.

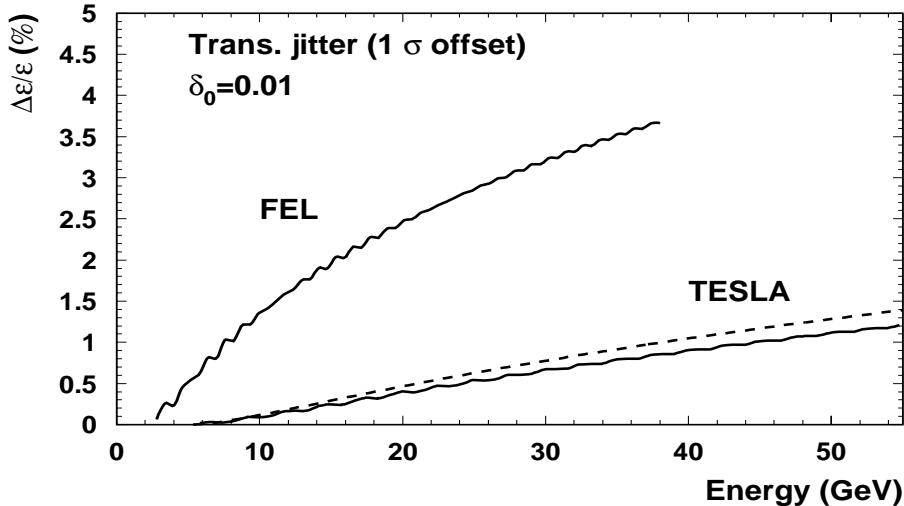


Fig.10 *The dispersive emittance dilution caused by injection jitter and initial uncorrelated energy spread. The beam performs free coherent oscillations with one sigma initial offset ($\sigma_T = 15\mu\text{m}, \sigma_F = 120\mu\text{m}$). The dashed line shows the analytical prediction for a collider beam in TESLA with the constant beta lattice ($\mu = 60^\circ$).*

3.3 Free coherent oscillations. Wakefield effects

A good analytical prediction of the emittance dilution by transverse wakefields is follow from the two-particle model of the bunch [6]. The beam is modeled by two macroparticles with the charge $Q/2$ that are separated by the longitudinal distance $\Delta s = 2\sigma_s$, where σ_s is the rms length of the bunch. The first, heading particle feels no transverse wakefield and thus undergoes free betatron oscillations with initial amplitudes y_0, y'_0 . The second, trailing particle experiences the dipole wakefields W_d due to the off-axis motion of the leading particle. The rms transverse spread of the particles σ_y is given by $\sigma_y^2 = \langle \Delta y^2 \rangle / 4$, where $\Delta y = y_2 - y_1$. With neglect of the correlated energy spread, the emittance enlargement of the bunch by transverse wake fields in the constant beta lattice machine is then given by [7]

$$\frac{\Delta\epsilon}{\epsilon}(z) = \frac{1}{2} \frac{a_0^2}{\epsilon_0} \left(\frac{eQW_d L_c}{8G} \right)^2 \frac{1}{\sin^2 \mu} \ln^2 \frac{\gamma(z)}{\gamma_0}, \quad (14)$$

where L_c is the focusing cell length, G is the acceleration gradient. The Green-function of the transverse wake potential for a TESLA cavity is given in Ref.[8].

The value of the transverse wake potential experienced by the trailing charge for TESLA beam is $W_D(2\sigma_s) = 16.6eV/pC/m^2$ and for FEL beam is $W_D(2\sigma_s) = 4.52eV/pC/m^2$.

Fig.11 shows the emittance dilution by wakefields for TESLA and FEL beams. The beams perform free coherent betatron oscillations with one standard initial offset ($a_0^2 = \varepsilon_0$). The tracking simulations include the correlated energy spread induced in accelerating sections due to the accelerating RF mode and the longitudinal wakefields. The rms correlated energy spread of the TESLA beam is $\delta_{corT} = 2.5 \cdot 10^{-4}$ (RF phase $\psi_s = 3.4^\circ$) and FEL beam $\delta_{corF} = 4 \cdot 10^{-4}$ (RF phase $\psi_s = 0$). Note, that the dominant effect for TESLA beam is the transverse wake, while the dilution of the FEL beam is dispersive due to correlated energy spread in the bunch and high phase advance per cell (form. 13). However, the emittance growth for both beams are below 1%.

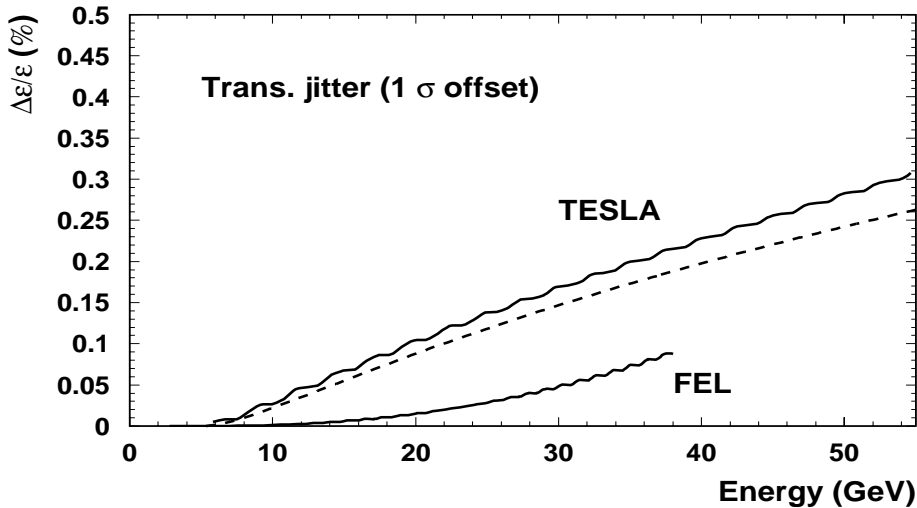


Fig.11 *The wakefield caused emittance dilution. The beam performs free coherent oscillations with one sigma initial offset. Dashed line -analytical prediction for TESLA beam.*

3.4 Accelerator section misalignments

The next source of the beam emittance dilution is the accelerating section misalignments. We again use the two-particle model of the bunch to evaluate the emittance dilution. In two-particle model, the difference in the transverse position of the head and tail particles $\Delta x = x_2 - x_1$ obeys the equation of motion

$$\Delta y'' + \frac{\gamma'}{\gamma} \Delta y' + K \Delta y = \frac{\gamma_0}{\gamma} C_w y_{ak} \quad (15)$$

with $C_w = eQW_D/2E_0$ and y_{ak} uncorrelated random misalignments of the cavities ($\langle y_{ak} y_{am} \rangle = 0, k \neq m$). Using M_{12} transport matrix element as the Green-

function, we obtain

$$\Delta y(z) = C_w \gamma_0 \sqrt{\frac{\beta(z)}{\gamma(z)}} \sum_{k=1}^N y_{ak} \int_{z_k}^{z_k+d_c} \sqrt{\frac{\beta(z')}{\gamma(z')}} \sin[\phi(z) - \phi(z')] dz' \quad (16)$$

where z is position along the linac, d_c is the cavity length, N is the cavity number. Using the model that the trailing particle experience the kick at the center of the cavity and replacing the beta function by its average value, the squared displacement averaged over the phase ϕ is then given by

$$\Delta \varepsilon = \frac{1}{4} \frac{\langle \Delta x^2(z) \rangle}{\beta(z)} = \frac{1}{8} \langle y_a^2 \rangle C_w^2 d_c^2 \frac{\gamma_0}{\gamma(z)} \sum_{k=1}^N \bar{\beta}_k \frac{\gamma_0}{\gamma_k} \quad (17)$$

Replacing the sum over the cavities by the integral in energy range, for constant beta lattice $\bar{\beta} = L_{cell}/\sin \mu$ we get

$$\frac{\Delta \varepsilon(z)}{\varepsilon} = \frac{\langle y_a^2 \rangle}{2N_{cav}\varepsilon_0} \left(\frac{eQW_D}{4G} \right)^2 \frac{\Delta \gamma}{\gamma_0} \frac{L_c}{\sin \mu} \ln \frac{\gamma(z)}{\gamma_0} \quad (18)$$

where ε_0 is the beam initial natural emittance, N_{cav} is the number of the cavities per single FODO cell. Fig.12 present the emittance dilution of the TESLA beam averaged over the 50 random samples of the cavity misalignments with the rms value $\sigma_{cav} = 0.5mm$. Note, that the same order of the emittance dilution is predicted if the modules (which contain 8 cavities) is misaligned by the rms value $\sigma_{mod} = 60\mu m$. The emittance dilution of the FEL beam due to cavity misalignments is in order $\Delta \varepsilon/\varepsilon \sim 10^{-5}$.

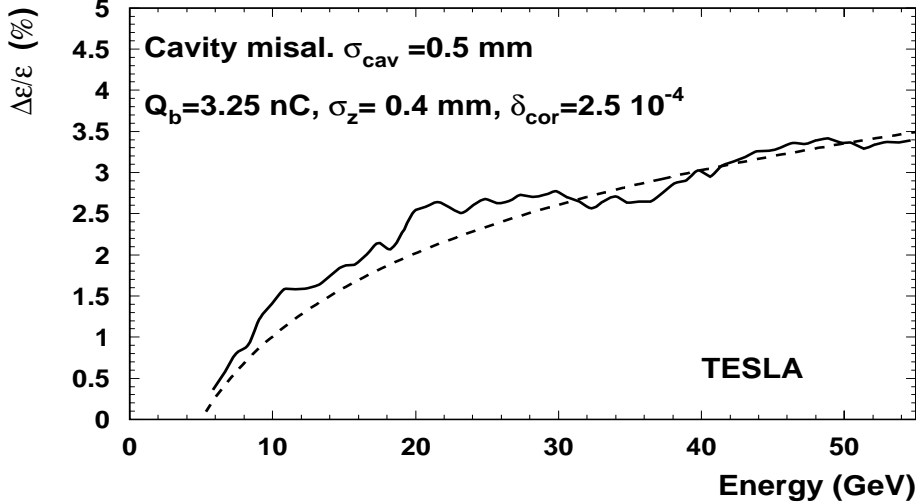


Fig 12. *Emittance dilution of the TESLA beam because of the cavity misalignments. Dashed line -analytical prediction.*

4 Trajectory correction

In this section some features of the beam dynamics in two beam operation mode of the TESLA are given when the quadrupoles are randomly misaligned. The study includes the one-to-one correction technique in single and two-beam operation mode. Some general aspects of the two-beam based alignment technique for the TESLA and FEL beams trajectory correction are discussed.

4.1 One-to-one correction

We assume that the trajectory is corrected to quadrupole centerlined trajectory in each F and D quadrupoles by the BPM measurements. The quadrupoles are randomly misaligned with the rms value σ_q , the BPM's also randomly misaligned with respect to quadrupole center with the rms value σ_b . In addition, the BPM's has the resolution with the rms expected value σ_r . Thus, after the complete one-to-one correction (minimization of the BPM measurements), the beam central trajectory $y_c(z)$ in quadrupoles is given by

$$y_{ck} = q_k + b_k + r_k \quad (19)$$

where q_k, b_k, r_k are random and uncorrelated values of quadrupole and BPM misalignments and BPM resolution. The central and off-energy trajectories are obey the equations of motion

$$y_c'' + \frac{\gamma'}{\gamma} y_c' + K(y_c - y_q) = G(z) \quad (20)$$

$$y'' + \frac{\gamma'}{\gamma} y' + K(1 - \delta)(y - y_q) = (1 - \delta)G(z) \quad (21)$$

where $G(z)$ is the bending function of corrector dipoles, $\delta(z)$ the relative energy deviation with respect to design energy. The difference orbit $\Delta y = y - y_c$ is then given by

$$\Delta y'' + \frac{\gamma'}{\gamma} \Delta y' + K(1 - \delta)\Delta y = \delta \cdot K(y_c - y_q) - \delta \cdot G(z) \quad (22)$$

Note, that the off-energy particle in misaligned structure not follow the linear dispersion trajectory but experience additional kick $\Delta y = \delta K y_c$ proportional to design corrected trajectory. The difference orbit is given by M_{12} transport matrix element and read as

$$\begin{aligned} \Delta y(z) = & \int_0^z \delta(z') K(z') y_c(z') M_{12}^\delta(z', z) dz' - \\ & - \int_0^z \delta(z') [K(z') y_q(z') + G(z') M_{12}^\delta(z', z)] dz' \end{aligned} \quad (23)$$

For small energy difference ($\delta \ll 1$) we can neglect the high order term $K\delta\Delta y$. By partial integration of the second term in the right hand side of the equation we then get

$$\Delta y(z) = \int_0^z \delta(z')K(z')y_c(z')M_{12}^\delta(z', z)dz' - \delta(z)y_c(z) - \int_0^z \delta'(z')y_c(z')dz' \quad (24)$$

It can be shown that the dominant contribution to emittance dilution is the first term of the right hand side. For initial uncorrelated energy spread δ_0 the actual energy spread in the bunch vary as $\delta(z) = \delta_0\gamma_0/\gamma$. The squared rms deviation of the off-energy particle averaged over the actual betatron phase and initial energy spread is then given by

$$\langle \Delta y^2(z) \rangle = \frac{1}{2} \langle y_c^2 \rangle \delta_{0rms}^2 \beta(z) \frac{\gamma_0}{\gamma(z)} \sum_n \frac{\gamma_0}{\gamma_n} K_n^2 L_{qn}^2 (\beta_{nmax} + \beta_{nmin}) \quad (25)$$

where $\langle y_c^2 \rangle = \langle \sigma_q^2 \rangle + \langle \sigma_b^2 \rangle + \langle \sigma_r^2 \rangle$. Using the well known relations for symmetric FODO lattice

$$\beta_{max} + \beta_{min} = \frac{2L_c}{\sin \mu}, \quad KL_qL_c = 4 \sin \frac{\mu}{2}, \quad (26)$$

the relative emittance dilution in thin lens approximation is then given by

$$\frac{\Delta \varepsilon}{\varepsilon} = 8\delta_{0rms}^2 \frac{\langle y_c^2 \rangle}{\varepsilon_0 L_c} \frac{\gamma_0}{\Delta \gamma} \tan \frac{\mu}{2} \cdot \ln \frac{\gamma(z)}{\gamma_0} \quad (27)$$

Fig.13 shows the dispersive emittance dilution for a TESLA beam, when the trajectory is corrected by one-to-one correction technique.

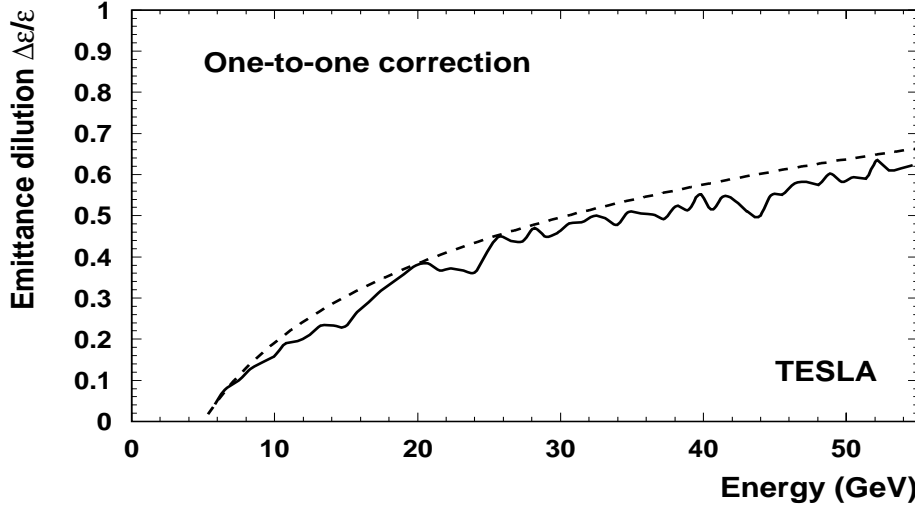


Fig.13 *Uncorrelated dispersive emittance dilution of the TESLA beam with one-to-one correction* ($\sigma_q = 100\mu m, \sigma_b = 100\mu m, \sigma_r = 10\mu m$). *Dashed line - analytical prediction.*

Note, that for high luminosity TESLA parameters, the uncorrelated dispersive emittance dilution is very large ($\delta_0 = 0.01$) even for the quadrupole and BPM misalignments at the level of $100\mu m$. In addition, in two beam operation mode, the coherent oscillations of the second beam not vanish and lead to large emittance dilution of the FEL beam.

4.2 Two beam operation

Let us consider the transverse dynamics of two beams with different energies in misaligned structure when the central trajectory one of the beams (let say high energy beam) is corrected by one-to-one correction technique. We assume that the ratio of initial energies is equal to ratio of acceleration gradients so that the ratio E_T/E_F is constant along the linac. The second beam (FEL beam) will then performs coherent oscillations according to

$$y_f = \frac{E_T}{E_F}y_t + \Delta y \quad (28)$$

where

$$\Delta y'' + \frac{\gamma_f'}{\gamma_f}\Delta y' + K_f\Delta y = -\bar{\delta}K_f y_t \quad (29)$$

with $\bar{\delta} = (E_T - E_F)/E_F$, y_t is the corrected TESLA beam trajectory, y_f is the trajectory of the FEL beam. Thus, for a large energy difference $\bar{\delta} \sim 0.4$, the second order dispersion trajectory of the FEL beam becomes the dominant, and the beam performs large coherent oscillation which depends on the random samples of quadrupole and BPM misalignments

$$\Delta y = -\bar{\delta} \int_0^z K_f(z')y_t(z')M_{12}^F(z', z)dz' \quad (30)$$

Note that the oscillations of the FEL beam around the linear dispersion trajectory is essentially adequate to beam coherent oscillation in misaligned structure without the trajectory correction. Evaluating the integral we obtain

$$\Delta y(z) = -\bar{\delta} \sqrt{\frac{\beta(z)}{\gamma(z)}} \sum_k y_{tk} K_{fk} L_q \sqrt{\beta_k \gamma_k} \sin[\phi(z) - \phi(z_k)] \quad (31)$$

For squared displacement only the correlated members should be taken into account and we get

$$\langle \Delta y^2 \rangle = \bar{\delta}^2 \langle y_t^2 \rangle \frac{\beta(z)}{\gamma(z)} \sum_k K_{fk}^2 L_q^2 \beta_k \gamma_k \sin^2[\phi(z) - \phi(z_k)] \quad (32)$$

The additional rms contribution to FEL disturb trajectory is then given by

$$\gamma_y \langle \Delta y^2 \rangle + 2\alpha_y \langle \Delta y \Delta y' \rangle + \beta_y \langle \Delta y'^2 \rangle = A^2 \quad (33)$$

where

$$A^2 = \bar{\delta}^2 \langle y_t^2 \rangle \frac{1}{\gamma(z)} \sum_k K_{fk}^2 L_q^2 \beta_k \gamma_k \approx 8\bar{\delta}^2 \frac{\langle y_t^2 \rangle}{L_c} \frac{\gamma_0}{\Delta\gamma} \tan \frac{\mu}{2} \left[\frac{\gamma}{\gamma_0} - \frac{\gamma_0}{\gamma} \right] \quad (34)$$

The parameters in formula are related to FEL beam . Thus, the rms disturb phase ellipse of the FEL beam is grow linearly with energy leading both to large dispersive and wakefield emittance dilution. Fig.14 shows the coherent FEL beam oscillations in the main linac when the TESLA beam is corrected to quadrupoles centers by one-to-one correction technique. Quadrupole misalignments $\sigma_q = 0.5mm$, the BPM misalignments $\sigma_b = 0.1mm$ with the resolution $\sigma_r = 10\mu m$. Actually, it becomes impossible to run the machine with the one-to-one trajectory correction of one of the beams keeping small the amplitude of coherent oscillations of the second beam.

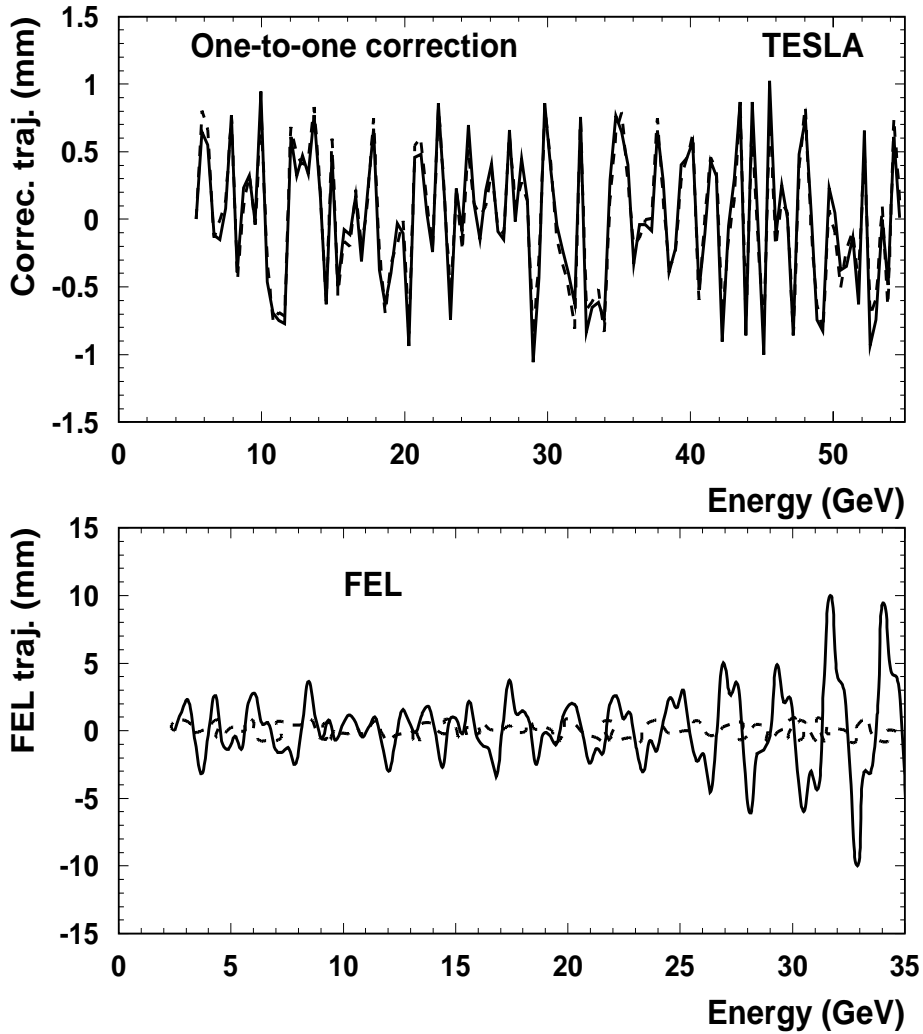


Fig.14 The TESLA beam corrected trajectory (one-to-one correction, $\sigma_q = 0.5mm$, $\sigma_b = 0.1mm$, $\sigma_r = 10\mu m$) and the coherent oscillations of the FEL beam.

4.3 On the two beam based trajectory correction

The TESLA design with the integrated FEL beam opens the possibility to use the information on the trajectory of two beams with different energies to minimize the difference orbit by the fitting the strength of the corrector dipoles. The procedure is essentially similar to beam based trajectory correction algorithm [9, 10].

To correct the difference orbit resulting from changing the effective energy, we need to measure the TESLA and FEL beam trajectories. If we only consider transverse deflections due to quadrupole misalignments and dipole correctors, the k -th BPM will measure

$$m_{Tk} = r_k(t_1) + b_k + \sum_{l=1}^{k-1} \theta_l M_{12}^t(z_l, z_k), \quad (35)$$

$$m_{Fk} = r_k(t_2) + b_k + \sum_{l=1}^{k-1} \frac{E_{Tk}}{E_{Fk}} \theta_l M_{12}^f(z_l, z_k) \quad (36)$$

where θ is the integrated deflection of the dipole correctors and the quadrupole misalignments. The difference orbit is then independent of the BPM's misalignments and is given by

$$\Delta m_k = [r_k(t_1) - r_k(t_2)] + \sum_{l=1}^{k-1} \theta_l \left[M_{12}^t(z_l, z_k) - \frac{E_{Tk}}{E_{Fk}} M_{12}^f(z_l, z_k) \right] \quad (37)$$

where $M_{12}^{t,f}$ is transport matrix element for TESLA (t) and FEL (f) beams. Then, in principal, we could solve the equation for the N_q unknown quadrupole misalignments, provided that the BPM precision errors and any unknown deflections are negligible. However, the BPM precision errors will limit the accuracy with which we can correct the difference orbit.

The detail study of the correction procedure based on the difference orbit analyzes including all the errors is beyond the scope of this report. We discuss some general features that is related to the real beam trajectories when the correction is based on the minimization of the difference orbit. Note, that including the BPM precision errors, the solution for difference orbit could be reduced at the level of the BPM precision errors. However, the minimization of the difference orbit still not provides the reduction of the real trajectories at the level of BPM precision errors. Indeed, from (28),(30) we can write for the difference trajectory

$$\bar{\delta} y_t(z) - \bar{\delta} \int_0^z K_f(z') y_t(z') M_{12}^f(z', z) dz' = \bar{r}(z) \quad (38)$$

where $\bar{r}(z)$ is the some interpolation function for the difference orbit, provided that $\bar{r}(z_k) = r_k(t_1) - r_k(t_2)$ at the k -th quadrupole. Assuming that the BPM's have random precision errors with rms value σ_r , the measured difference orbit will

differ from the actual difference orbit by an rms error $r_{rms} = \sqrt{2}\sigma_r$. In smooth focusing model we could rewrite the expression for the difference orbit as

$$y_t(z) - k_f \int_0^z y_t(z') \sin[k_f(z - z')] = \frac{\bar{r}(z)}{\bar{\delta}} \quad (39)$$

For simplicity, the beam acceleration is not taken into account. Using Laplace transform, we get

$$Y_t(p) = \bar{\delta}^{-1} \left(1 + \frac{k_f^2}{p^2} \right) \mathcal{L}[\bar{r}(z)]. \quad (40)$$

The waiting trajectories for the TESLA and FEL beams is then given by

$$y_t(z) = \bar{\delta}_f^{-1} \left[\bar{r}(z) + k_f^2 \int_0^z \int_0^{z'} \bar{r}(z'') dz'' dz' \right], \quad (41)$$

$$y_f(z) = \bar{\delta}_t^{-1} \left[\bar{r}(z) + k_t^2 \int_0^z \int_0^{z'} \bar{r}(z'') dz'' dz' \right], \quad (42)$$

with $\bar{\delta}_{t,f} = \Delta E/E_{t,f}$, $\Delta E = E_t - E_f$, and $k_{t,f}$ the betatron wave numbers for TESLA and FEL beams respectively. The real trajectories of the beams at the n -th quadrupole is then given by

$$y_t(z_n) = \bar{\delta}_f^{-1} \left[\bar{r}_n + k_f^2 D^2 \sum_{k=1}^{n-1} \sum_{m=1}^k \bar{r}_m \right] \quad (43)$$

$$y_f(z_n) = \bar{\delta}_t^{-1} \left[\bar{r}_n + k_t^2 D^2 \sum_{k=1}^{n-1} \sum_{m=1}^k \bar{r}_m \right] \quad (44)$$

where D is the distance between two quadrupoles. Note, that the difference orbit is at the level of BPM's precision errors $y_t - y_f = \bar{r}_n = r_n(t_1) - r_n(t_2)$. Taking into account that $\langle \bar{r}_n \bar{r}_k \rangle = 0$ if $n \neq k$, for waiting rms trajectories of the TESLA and FEL beams we get

$$\langle y_t^2(z) \rangle^{1/2} \sim \langle y_f^2(z) \rangle^{1/2} \sim \frac{E_t}{\Delta E} \sigma_r k_t^2 D z \quad (45)$$

The beam acceleration is not change the essential of the situation. The real trajectories are diverge from the linac centerline and the waiting rms trajectories of the TESLA and FEL beams grow approximately linear with the beam energy. This occurs because the difference orbit is not referenced to the linac centerline and small errors add. Thus we need to include some information about the real trajectory while correcting the difference orbit.

The well established procedure [10] is to perform a least squares solution for the unknowns, using both the original trajectory and the difference orbit weighted with the absolute accuracy with which these trajectories are known. The dipole corrector strengths are then minimize the sum

$$\sum_k \frac{(m_{Tk} + y_{Tk})^2}{\sigma_r^2 + \sigma_b^2} + \frac{(\Delta m_k + \Delta y_k)^2}{2\sigma_r^2} \quad (46)$$

Thus, we suppose, that the minimization of the both difference orbit and original TESLA trajectory will provides the correction of the both TESLA and FEL beam trajectories at the level of the BPM resolution.

An uncorrelated dispersive emittance dilution of the beams is then given by the BPM resolution only and is predicted as

$$\frac{\Delta\varepsilon}{\varepsilon} = 16\delta_{0rms}^2 \frac{\sigma_r^2}{\varepsilon_0 L_c} \frac{\gamma_0}{\Delta\gamma} \tan \frac{\mu}{2} \cdot \ln \frac{\gamma(z)}{\gamma_0} \quad (47)$$

Fig.15 shows the dispersive emittance dilution of the TESLA beam when the trajectories of the both beams is corrected at the level of the BPM resolution ($\sigma_r = 10\mu m$) with respect to linac centerline assuming that the initial jitter is zero. The dilution of the FEL beam is at the level of 10^{-4} ($\delta_0 = 0.01$).

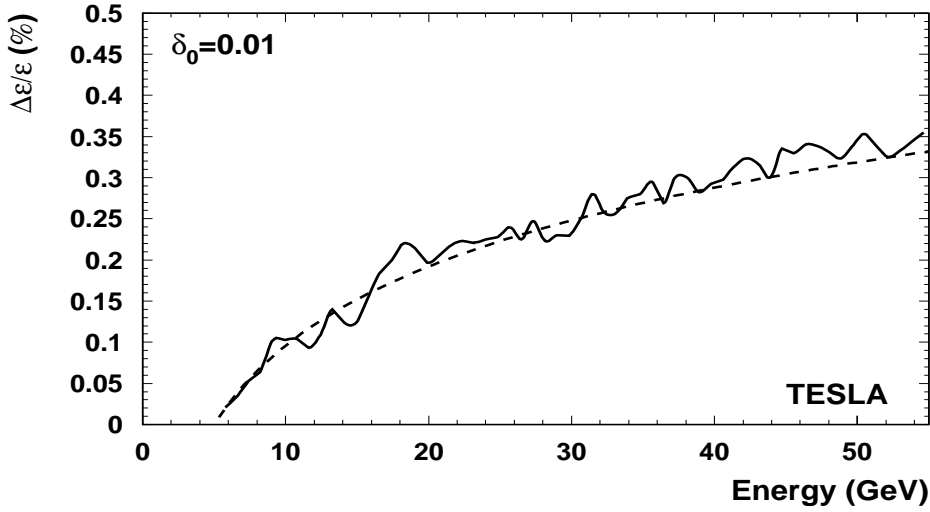


Fig.15 The uncorrelated dispersive emittance dilution of the TESLA beam with the two-beam based trajectory correction. Dashed line -analytical prediction.

To predict the emittance dilution caused by the wakefields, we assume that the off- axis trajectory of the beam in accelerating sections is given by $y_{off} = (y_F + y_D)/2$ with the rms expected value $\langle y_{off}^2 \rangle = \sigma_r^2$. The predicted emittance dilution is then given by

$$\frac{\Delta\varepsilon(z)}{\varepsilon} = \frac{\sigma_r^2}{4\varepsilon_0} \left(\frac{eQW_D}{4G} \right)^2 \frac{\Delta\gamma}{\gamma_0} \frac{L_c}{\sin \mu} \ln \frac{\gamma(z)}{\gamma_0} \quad (48)$$

The emittance dilution of the TESLA beam by the transverse wakefields is presented in Fig.16, when the trajectories of the both beams corrected to linac centerline with the accuracy of the BPM precision $\sigma_4 = 10\mu m$. The emittance dilution of the FEL beam is at the level of 10^{-5} .

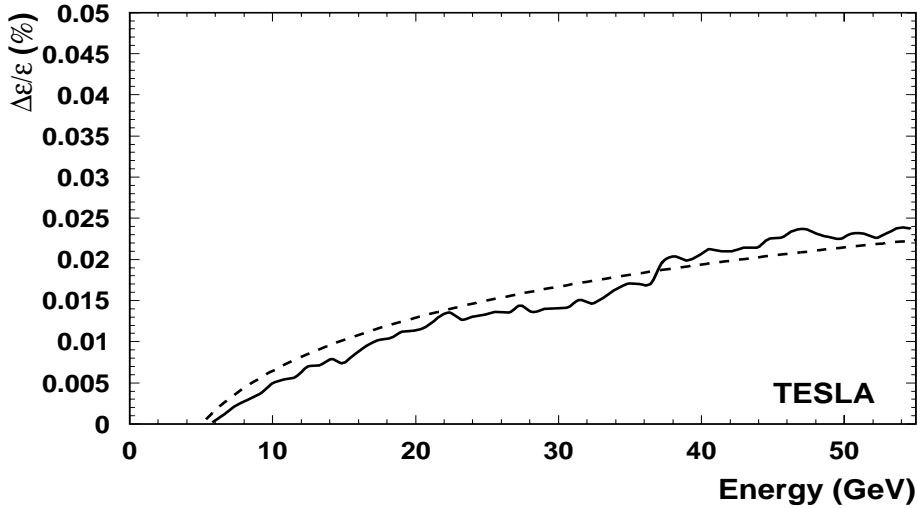


Fig.16 The wakefield emittance dilution of the TESLA beam with the two-beam based trajectory correction. Dashed line -analytical prediction.

5 Summary

The main aspects of the beam dynamics in two-beam operation mode of the TESLA have been studied. The basic conclusions are follow:

- * the use of the one-to-one correction technique for one of the beams accompanies by the large coherent oscillations of the second beam ;
- * the two-beam operation part of the main linac need to be straight to prevent the dispersion caused errors for beam based correction technique;
- * the emittance preservation of the both beams at the level of 1% can be provided by using the two beam based trajectory correction technique.

Although the results of our study gives very promising result for emittance preservation of the both TESLA and FEL beams, there are need a complete study of the beam based trajectory correction technique including the effects caused by the beam jitter, field errors and the date analyzes.

Acknowledgments

The author thanks Reinhard Brinkmann and Joerg Rossbach for many helpful and stimulating discussions on the topic of the report. Special thanks to Gerhard Soehngen and Dieter Trines for the permanent support of the work.

References

- [1] *Conceptual Design of a 500 GeV e^+e^- Linear Collider with Integrated X-Ray Laser Facility*, edited by R. Brinkmann, G. Materlik, J. Rossbach and A. Wagner, Hamburg, DESY 1997-048, 1997.
- [2] P.J. Bryant, Proc. of the 1992 CERN Accel.School, CERN 94-01,1994.
- [3] R.Brinkmann”High Luminosity TESLA-500”, TESLA 97-13, 1997.
- [4] W. Decking , TESLA Meeting, TESLA 99-13, 1999.
- [5] M. Sands, ”Emittance Growth from Radiation Fluctuations”, SLAC-AP-47 (1985).
- [6] P.Wilson in *Physics of High Energy Particle Accelerators*, edited by R.A.Carrigan, F.R. Huson, and M. Month, AIP Conf. Proc. No. 87, (AIP, New York, 1982), Sec. 11.1.
- [7] K. Bane, Report No. SLAC-PUB-4169, 1986.
- [8] A.Mosnier, A.Novokhatsky, DAPNIA/SEA-9608, 1996.
- [9] C.E. Adolphsen etc, SLAC-PUB-4902, March 1989.
- [10] T.O. Raubenheimer and R.D. Ruth, NIM (A), **302**, 191 (1991)